A Study of the Rheological Behavior of High-Temperature Polymer Electrolyte Membrane Solutions

Tequila A. L. Harris,[1] Daniel Walczyk[2]

[1]*Georgia Institute of Technology, Atlanta Georgia, The George W. Woodruff School of Mechanical Engineering, Atlanta, Georgia*
[2]*Rensselaer Polytechnic Institute, Department of Mechanical, Aerospace, and Nuclear Engineering, Troy, New York*

Received 14 March 2008; accepted 8 August 2008
DOI 10.1002/app.29166
Published online 22 October 2008 in Wiley InterScience (www.interscience.wiley.com).

ABSTRACT: The viscosity behavior of various compositions of polymer electrolyte membrane solutions, which are later hydrolyzed into proton conducting membrane film for fuel cells, is characterized. Using the Carreau-Yasuda model and time–temperature superposition, an empirical model relating the viscosity as a function of temperature and shear strain rate has been developed for several membrane solution compositions. It is observed that the viscosity of the non-Newtonian membrane has a strong correlation to the membrane's inherent viscosity (a property determined during membrane synthesis). © 2008 Wiley Periodicals, Inc. J Appl Polym Sci 111: 1286–1292, 2009

Key words: rheology; membrane; viscosity; modeling

INTRODUCTION

In response to a looming energy crisis, researchers have pursued numerous strategies to develop reliable alternative energy techniques, such as fuel cells. Of particular interest are high-temperature polymer electrolyte membrane (PEM) fuel cells. Novel classes of high-temperature PEMs are being developed around the world including: Sandia Polymer Electrolyte Alternative, which operates at temperatures up to 140°C[1]; organically modified silicates, developed by the National Aeronautics and Space Administration, which have shown good proton conductivity at temperature up to 120°C[2]; commercial polyetheretherketone has been sulfonated and reacted with $SiCl_4$ to form a hybrid polymer which has shown high conductivity for PEMs[3] at the University of Provence, France; diamine bearing sulfophenyl pendant groups of 2,20-(4-sulfophenyl) benzidine have been synthesized successfully exhibiting reasonably high conductivity for low temperature PEM fuel cell applications[4]; and membranes consisting of polybenzimidazole (PBI)[5] doped with polyphosphoric acid (PPA),[6,7] which operate at temperatures above 120°C and have shown good conductivity and stability. Furthermore, extensive research has been conducted to develop PEM with increased performance, longevity, and durability.[6,8–16] A major issue with polymer solutions in general, and the new classes of PEM formulations is that synthesis is not trivial, as slight variations in chemical composition can have a significant impact on the membrane's physical and mechanical properties.[6] It has been shown that the mechanical strength of polymer electrolyte films vary widely depending on the solute content.[17] In addition to conducting protons, the PEM acts also as a gas separation barrier for the hydrogen and oxygen. It has been shown that for the formation of thin porous membrane film a broad molar mass distribution is most favorable.[18] Furthermore, it has been shown that the rheological properties of hollow fiber membranes influence the membrane performance for capturing CO_2.[19]

Characterization of the rheological behavior of new classes of PEMs is typically conducted before membrane manufacturing, such that an appropriate process can be developed based on the flow behavior of the solution. This important step is typically not conducted during the development/synthesis stage of the membrane solution, but is an afterthought, handled at the manufacturing stage.[20,21] The flow behavior of the fluid as a function of temperature and shear strain rate is critical for manufacturing purposes, because this parameter controls the thickness and distributed uniformity of the fluid as it is cast onto a substrate. In particular, knowing the rheological properties (especially viscosity) allows for development of membrane production system capable of handling variations in PEM compositions,

Correspondence to: TequilaA. L. Harris (tequila.harris@me.gatech.edu).

Contract grant sponsors: Clare Booth Luce Foundation, Center for Automation Technologies and Systems at Rensselaer Polytechnic Institute, BASF Fuel Cell, GmbH.

which the authors believe is important, due to the myriad of compositions of membrane solutions currently being developed for the fledgling fuel cell industry. The PEM solution of particular interest in this article arguably is a worst case scenario in terms of handling and processing, in that it is highly corrosive, viscous with high temperature- and strain-rate dependency, tacky, and susceptible to the environment.[7,20] Thus, from a process development standpoint, it is an extremely difficult material to handle and understanding the rheological behavior is of great importance.

This article discusses how the rheological behavior of the PEM solution developed by Xiao et al.[7] (henceforth called PBI/PA solution) was experimentally characterized and presents several empirical rheological models related to various compositions of the PBI/PA solution. These PEM solutions exhibit significant changes in rheological behavior depending upon chemical composition.[20] The empirical models, which predict the viscosity of the PEM solution as a function of temperature and shear strain rate, are developed by coupling the Carreau-Yasuda Model and time–temperature superposition, which is discussed in detail in the succeeding sections. For manufacturing purposes, characterizing the solution's rheological properties for varying process conditions is essential, because the PBI/PA membrane solution is not formulated for a specific surface application technique, but rather for its operational performance in a fuel cell stack. Also, knowing the rheological behavior of the material will provide critical data for the temperature and shear strain rate sensitivity of the fluid, so that the manufacturer can predict the volumetric flow rate of the fluid, which directly impacts the thickness and uniformity of the membrane. In addition, the PEM solution must stabilize or recover quickly after casting into a film to avoid undesirable spreading or flow in unintended locations on a substrate or other surrounding components.

CARREAU-YASUDA AND TIME–TEMPERATURE SUPERPOSITION MODELS

For this work, the authors chose to use Carreau Yasuda and time–temperature superposition models to empirically describe the behavior of complex polymer materials. Non-Newtonian behavior (i.e., temperature and shear strain rate dependency) can be easily modeled by coupling these models. This is important due to the sensitive nature of not only the PBI/PA solution but also the manufacturing process. As the PBI/PA solution flows through the manufacturing tool, it will be subjected to shear strain. In addition, the PBI/PA solution has a strong dependence on temperature. As such, an empirical viscosity model as a function of shear strain rate and temperature for each composition of the PBI/PA solution is desired. The empirical models will be incorporated into an overall system model, which describe the flow behavior of the fluid at any point in a system, allowing for real-time automation adjusts for a continuous processing system to ensure uniform film deposition.

The Carreau-Yasuda model provides viscosity (η, Pa s) as a function of shear strain rate ($\dot{\gamma}$, s^{-1}) for a specific temperature.[22] Shear strain rate is also the rate of change of velocity at which one layer of fluid passes over an adjacent layer. The Carreau-Yasuda model is expressed by the following relationship:

$$\frac{\eta - \eta_\infty}{\eta_0 - \eta_\infty} = [1 + (\dot{\gamma}\lambda)^a]^{\frac{n-1}{a}}. \quad (1)$$

The parameters used in this model including an explanation of the effect that each parameter has on the curve fit to the viscous materials rheological behavior are discussed later.[22]

η–the viscosity of the fluid.

η_∞–the viscosity function approaches the constant value η_∞ as $\dot{\gamma}$ increases.

η_0–the viscosity function approaches η_0 as $\dot{\gamma}$ decreases.

a–this exponent affects the shape of the transition region between the zero-shear-rate plateau and the rapidly decreasing (power-law like) portion of the viscosity versus shear rate curve. Increasing *a* sharpens the transition.

λ–the parameter is a time constant for the fluid. The value of λ determines the shear rate at which the transition occurs from the zero-shear-rate plateau to the power-law portion. It also governs the transition from power-law to $\eta = \eta_\infty$.

n–This factor is a power-law-like parameter that describes the slope of the rapidly decreasing portion of the η curve.

It is clear that a disadvantage of using this model is that five parameters must be fit to a curve simultaneously; as such, the accuracy of the empirical solution will depend upon the method used to curve fit the numerical data. Figure 1 illustrates how *n*, *a*, and λ affect specific portions of the analytical η versus $\dot{\gamma}$ curve plotted on log–log axes.

For non-Newtonian fluids, the viscosity at infinity, η_∞, occurs as the shear strain rate approaches infinity and the viscosity approaches zero. Because η_∞ is much less than η_0, it is often neglected, as is the case for this study. As such, setting η_∞ to zero, eq. (1) reduces to the following form:

$$\frac{\eta}{\eta_0} = [1 + (\dot{\gamma}\lambda)^a]^{\frac{n-1}{a}}. \quad (2)$$

For many viscous fluids, the series of η versus $\dot{\gamma}$ curves for various temperatures can be reduced

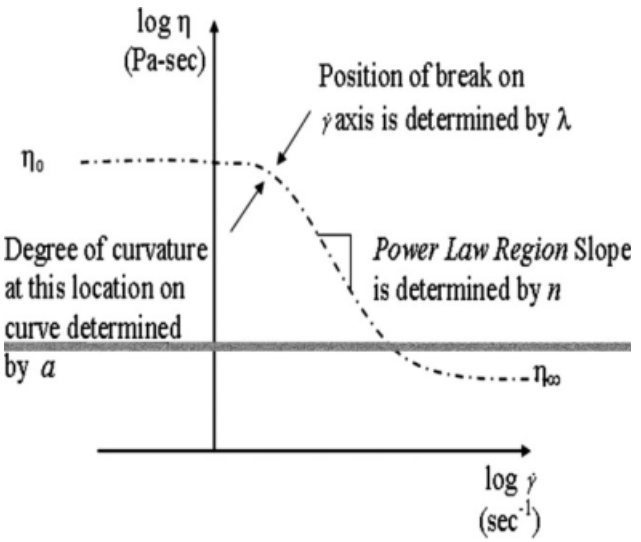

Figure 1 Illustration of the effects of various parameters in the Carreau-Yasuda model.

down to a single "Master Curve" by applying a shift factor a_T. Specifically, for each individual temperature curve, the viscosity is divided by a_T, and the shear strain rate is multiplied by a_T, thereby creating a reduced viscosity versus reduced shear rate curve. The reduced viscosity ($\frac{\eta}{a_T}$) versus reduced shear rate ($a_T\dot{\gamma}$) data superimposed on each other can be curve fit by a single "Master Curve." The Master Curve is basically a curve fit to all of the reduced η versus $\dot{\gamma}$ curves. This technique is known as "Time–Temperature Superposition."[23,24] The general concept is illustrated in Figure 2. All of the "shifted" curves will ideally lie on the same Reference Curve, which is valid for a membrane material of a particular chemical composition. If this is the case, then eq. (2) takes on the following form:

$$\frac{\eta}{a_T} = \eta_0[1 + (a_T\dot{\gamma}\lambda)^a]^{\frac{n-1}{a}}. \quad (3)$$

The Arrhenius approach is used to solve for the shift factor a_T, shown in eq. (4). The Arrhenius form is used due to its accuracy for predicting temperature dependence of the rate constant, which will be substituted into the final empirical model. The relationship of a_T to the inverse absolute temperature (K^{-1}) is shown in eq. (4). An exponential curve fit yields an accurate equation relating a_T to the absolute temperature, and a_T is obtained by trial and error until each of the shifted curves fit to the Reference Curve:

$$a_T = c_1 e^{\frac{c_2}{T}} \quad (4)$$

where c_1 and c_2 are dimensionless constants. By substitution, an empirical viscosity model that is temperature and shear rate dependent is developed, yielding eq. (5), a complete viscosity model that is temperature and shear strain rate dependent.

$$\eta = \eta_0 c_1 e^{\frac{c_2}{T}}\left[1 + \left(c_1 e^{\frac{c_2}{T}}\dot{\gamma}\lambda\right)^a\right]^{\frac{n-1}{a}}. \quad (5)$$

To develop the empirical Carreau-Yasuda models for different PBI/PA membrane solutions, first, all the temperature-dependent η versus $\dot{\gamma}$ curves are superimposed, creating a Master Curve. Then, η_0 is estimated by the left-most horizontal part of the Master Curve. Next, a curve is fit to the a_T versus the absolute temperature of the η versus $\dot{\gamma}$ curves to establish a governing equation between a_T and absolute temperature T (in Kelvin), which is then substituted for a_T. Finally, the Carreau-Yasuda equation parameters are obtained by observation (i.e., η_0), trial and error, or a unique program (i.e., n, a, and λ) and are fit to the Master Curve. The initial guess for a is typically two.[25] To obtain an initial guess for n, a power-law curve is fit to the Master Curve, where n is the power-law exponent in the following expression $\eta = k\dot{\gamma}^{n-1}$, and k is the consistency index (Pa s^n). n, a, and λ are finally substituted into the equation resulting in an empirical Carreau-Yasuda model.

As discussed in detail previously, the first step in developing an empirical Carreau-Yasuda Model is generating a "Master Curve" for the PBI/PA membrane solutions, using the raw data. A program written in Matlab Simulink 7.0.2 has been developed, which automatically shifts each of these viscosity curves, using a shift factor a_T, to an arbitrarily chosen η versus $\dot{\gamma}$ Reference Curve (e.g., η versus $\dot{\gamma}$ at 120°C), by using the fminsearch function. Other key parameters (i.e., n, a, and λ) are also determined, using a code developed in Matlab Simulink. Because of the number of parameters being fit some error

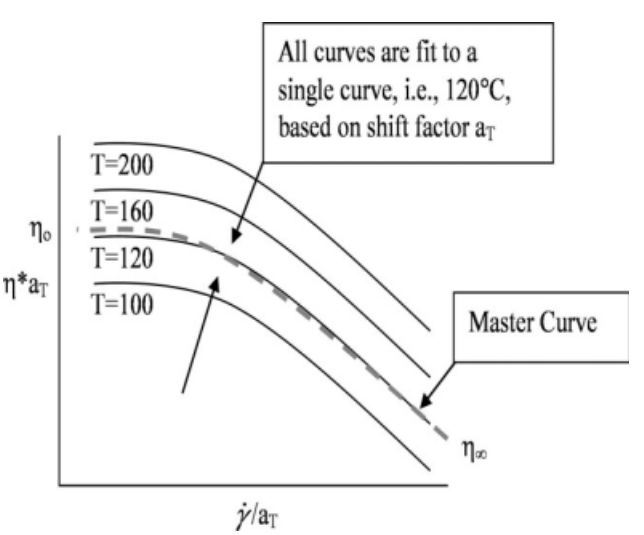

Figure 2 Schematic of a Master Curve.

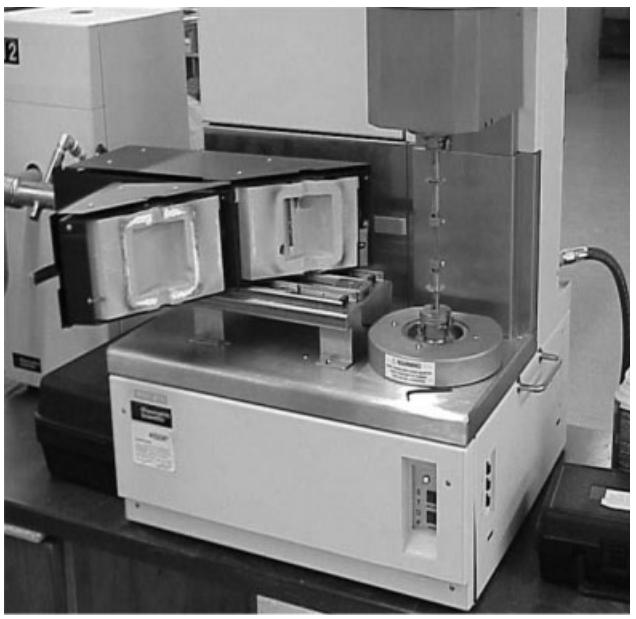

Figure 3 Rheometric Scientific RDA III Mechanical Analyzer.

will exist, especially as the viscosity approaches zero; however, this method has been found to be a good approximation for the models developed.

The remainder of this article describes the experimental setup and procedure for rheological characterization of various PBI/PA membrane compositions followed by an explanation of how the empirical models, based on the Carreau-Yasuda model, are developed.

EXPERIMENTAL

To characterize the behavior of the PBI/PA solution, rheology experiments for the PBI/PA membrane solution were conducted using a Rheometric Scientific RDA III Mechanical Analyzer, shown in Figure 3. The parallel plate configuration shown in Figure 4 was used to contain the solution during each experiment. Because the viscosity of the material is higher at lower temperatures, a small diameter upper plate (25 mm) and larger diameter lower plate (40 mm), which had a raised outer edge to form a cup, was used. This plate geometry helps to prevent the highly corrosive membrane solution from splattering out radially onto the test equipment as the upper plate rotates, especially as the fluid viscosity decreases at higher temperatures. To characterize the rheological behavior, the solution is tested by measuring the absolute viscosity (η) versus shear rate ($\dot{\gamma}$) of the PBI/PA membrane solution for possible casting temperatures in the range of 80 to 200°C.

Experimental procedure

The viscosity of the PBI/PA membrane solutions was measured at various temperatures and shear rates using the mechanical analyzer. The temperature was set initially at 80°C and a complete shear rate sweep (i.e., 0.1–100 s^{-1}) in increments of 5 data points/decade was performed. This test was repeated for other temperatures including 100, 120, 140, 160, 180, and 200°C, two or three times each. Because of the limitations of the test equipment, shear rates higher than 200 s^{-1} were not realizable. Throughout the duration of the experiment, the membrane solution was kept in a nitrogen atmosphere so that the sample did not prematurely hydrolyze due to exposure to moisture in the air.

Experimental characterization

The PBI/PA solution used in this study is synthesized (manufactured) by BASF Fuel Cell GmbH and used as received. Each nitrogen-purged 1 L bottle of solution was stored in a sealed plastic container to limit its exposure to varying environmental conditions (e.g., humidity, temperature, etc.) prior to casting it into a membrane. It is important to note that a critical assumption is the solution is homogeneously mixed.

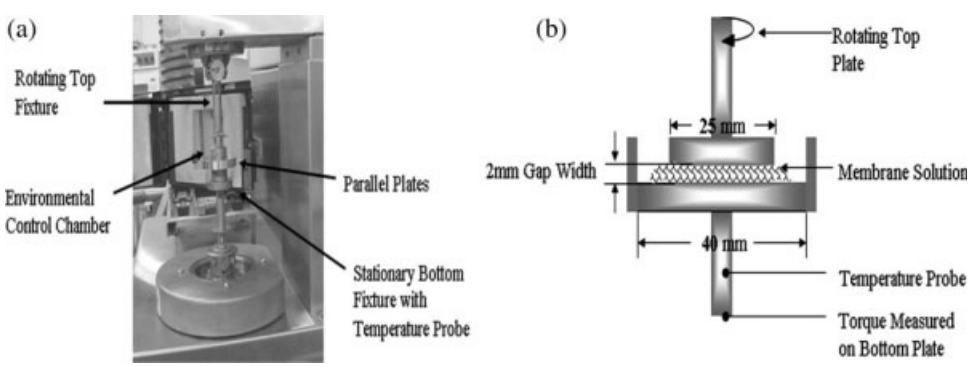

Figure 4 (a) Picture of mechanical analyzer plate fixtures with parallel plates installed and a (b) schematic of a cross-sectional view for the parallel plates.

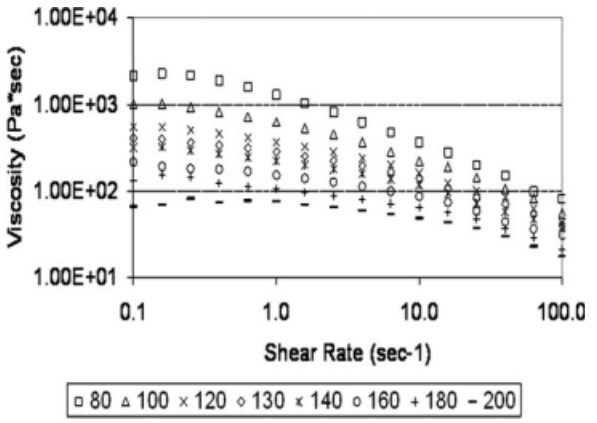

Figure 5 Experimental data for PBI/PA solution of IV 4.0 at 120°C.

The inherent viscosity (IV) of each PBI/PA composition was predetermined by the manufacturer to be 4.0, 4.75, 5.0, 5.3, and 5.4 dL/g, which is inherent to the synthesis process. The IV (η_{IV}) is the ratio of relative viscosity – the ratio of the solution viscosity η to the solvent's viscosity, which in this case is PPA – to the mass concentration of the polymer expressed as

$$\eta_{IV} = \frac{\ln\ \eta_{relative}}{C} = \frac{\ln\left(\frac{t_{solution}}{t_{solvent}}\right)}{C} \quad (7)$$

where $\eta_{relative}$ is the relative viscosity, C is the polymer solution concentration in g/dL, $t_{solution}$ is the average solution flow time in seconds, and $t_{solvent}$ is the average solvent flow time.[26] For the author's purposes, the value for a particular membrane IV is used to refer to different membrane solutions throughout the remainder of this article, and in such cases, the units will be omitted (e.g., IV 4.75).

EXPERIMENTAL RESULTS: VISCOSITY VERSUS SHEAR STRAIN RATE CURVES

The viscosity versus shear strain rate curves for each of the PBI/PA membrane solution compositions are presented in this section based on data using the experimental setup previously described. For each PBI/PA composition, a shear strain rate sweep from 0.01 to 100 s^{-1} was conducted for a temperature range for 80–200°C, and the corresponding viscosity data plotted on log–log axes is shown on a typical graph in Figure 5. Each set of data curves will be used to develop the corresponding empirical viscosity model as a function of shear strain rate and temperature, based on the Carreau-Yasuda model and time–temperature superposition.

All five of the different PBI/PA membrane solutions that were tested exhibit non-Newtonian fluid behavior. In addition, as shear strain rate approaches zero, the viscosity appears to reach a steady condition, so the viscosity at zero shear (η_0) can be reasonably assumed. Because the behavior of the PBI/PA membrane solution could not be easily characterized at very high shear rates, it is assumed that at sufficiently high shear strain rates the viscosity will be approach zero.

Analysis of membrane solution using Carreau-Yasuda's Model

Using the experimental data shown in Figure 5, an empirical model is developed for each membrane composition. First, the experimental data is shifted to a Reference Curve, i.e., 120°C, as shown in a typical graph in Figure 6 as thin solid lines. Then, a Master Curve is fit to the shifted curves, thereby providing a final empirical curve fit shown as a heavy solid line on Figure 6. The corresponding n, a, and λ parameters (Carreau-Yasuda model) for each PBI/PA membrane solution, in addition to the shift factor a_T are included in Table I. Plotting a_T with respect to inverse absolute temperature (K^{-1}), as shown in Figure 7, and fitting a curve to the results is an important step in developing the empirical viscosity model for each solution. The curve-fit equation, for a_T, is then substituted into eq. (5), thereby providing a direct correlation with temperature. The corresponding a_T equation for each of the PBI/PA membrane solutions is shown in Table II.

Validation of empirical Carreau Yasuda models

A complete empirical viscosity model of the system as a function of temperature and shear rate, i.e.,

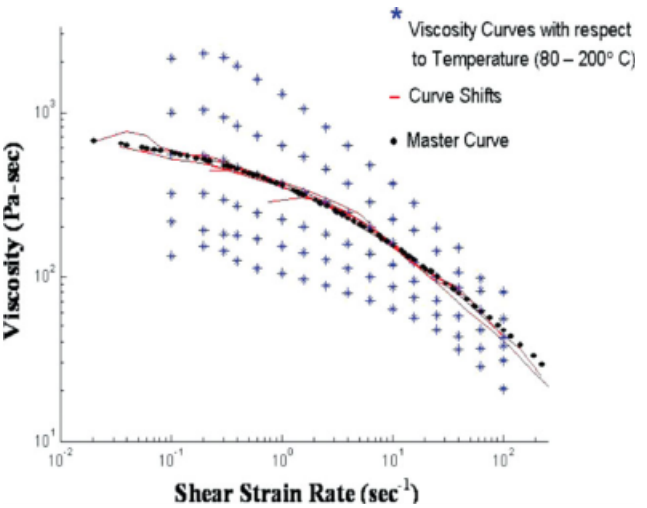

Figure 6 Carreau-Yasuda viscosity Master Curve and empirical curve for IV 4.0 at 120°C. [Color figure can be viewed in the online issue, which is available at www.interscience.wiley.com.]

TABLE I
Data for the Empirical Viscosity Curves of All Five PBI/PA Solutions That is Shifted to 120°C Including a_{Ti}, Where i = 1 to 7 of Corresponds to the Temperatures from 80–200°C in Increments of 20°C

	IV 4.0	IV 4.75	IV 5.0	IV 5.3	IV 5.4
a	0.442	0.7373	0.5211	0.2789	0.553
λ	0.4155	0.546	1.2105	0.0068	4.433
n	0.3136	0.4241	0.3492	−0.5458	0.3621
a_{T1}	7.5	4.5	9	4.75	8.5
a_{T2}	2.25	1.95	2	1.8	2
a_{T3}	1	1	1	1	1
a_{T4}	0.75	0.56	0.75	0.625	0.85
a_{T5}	0.55	0.35	0.54	0.4	0.57
a_{T6}	0.35	0.225	0.37	0.28	0.4
a_{T7}	0.2	0.16	0.26	0.2	0.3

$\eta = f(\dot{\gamma}, T)$, is developed by substituting the parameter values from Table I and the a_T curve-fit equations in Table II into eq. (5). The zero-viscosity (η_0) term is a constant that corresponds to the viscosity at very low shear rates, which is obtained while fitting the empirical curve to the Master Curve. The viscosity at infinity is assumed to be zero. The empirical models for each PBI/PA membrane solution are shown in Table III, where T_K is the absolute temperature.

To validate the accuracy of the empirical models, the model developed for IV 4.0 is evaluated at T_K = 160°C = 434°K and $\dot{\gamma} = 0.1\ s^{-1}$, and compared with the experimental data, presented in Figure 5. It is found that there is only 3.5% difference between the analytical solution (η = 208 Pa s) and the experimental value (η = 215.5 Pa s).

CONCLUSIONS

Several experiments are conducted to characterize the rheological properties for several PBI/PA membrane solution compositions, particularly viscosity. The Carreau-Yasuda and Time–Temperature Superposition models are used to develop empirical models for various compositions of the membrane solution, which directly correlates absolute viscosity, shear rate, and absolute temperature. The empirical models are useful for predicting the viscosity at any point in a system as a function of shear strain rate and temperature. Further studies are required to understand the ease and usefulness of using the empirical viscosity models to capture the flow behavior of the solution in real time.

From experimental data, it has been shown that the PBI/PA solution is non-Newtonian. Because the PBI/PA solution is non-Newtonian, it is important to maintain the processing temperature to negate undesired fluctuations in viscosity. It has also been shown that small changes in IV significantly affect the membrane solution's viscosity resulting in one or two orders of magnitude difference, for a given temperature. In general for the PBI/PA solution, it has been shown that higher the IV higher is the apparent viscosity, hence the PBI/PA solution's rheological behavior is highly dependent on a membrane solution's IV, for which additional research is needed. This study has shown that the difference in apparent viscosity between membrane solution with an IV of 4.0 and 5.4 is ~ 3000 Pa s at 80°C at a shear strain rate of 0.1 s^{-1}.

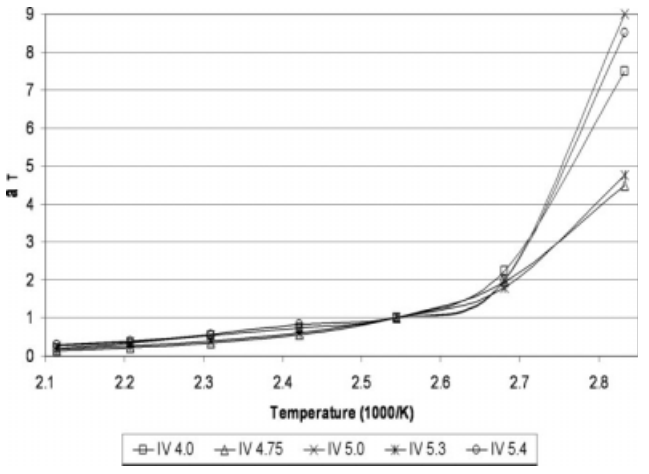

Figure 7 Curve fit of a_{Ti} values for all five PBI/PA solutions as a function of inverse absolute temperature (i.e., 1/K).

TABLE II
Curve-Fit Equations for a_T for Various PBI/PA Membrane Solutions Shifted to 120°C

PBI/PA solution IV	a_T Equation	Goodness of curve fit ratio (%)
4	$1 \times 10^{-5} \times e^{4.495/T}$	96.40
4.75	$8 \times 10^{-6} \times e^{4.63/T}$	99.60
5	$2 \times 10^{-5} \times e^{4.46/T}$	93.20
5.3	$2 \times 10^{-5} \times e^{4.271/T}$	98.80
5.4	$3 \times 10^{-5} \times e^{4.215/T}$	92.60

TABLE III
Empirical Viscosity Models for Various PBI/PA Membrane Solution Compositions

IV	Empirical viscosity models (η)
4.0	$\eta = 800 \times (1 \times 100^{-5} \times e^{(4.495\times1000/T_K)}) (1 + (0.416 \times 1 \times 10^{-5} \times e^{(4.495\times1000/T_K)})\dot{\gamma})^{0.442})^{(0.314-1)/0.442}$
4.75	$\eta = 375 \times (8 \times 10^{-6} \times e^{(4.630\times1000/T_K)}) (1 + (0.546 \times 8 \times 10^{-6} \times e^{(4.630\times1000/T_K)})\dot{\gamma})^{0.737})^{(0.424-1)/0.737}$
5.0	$\eta = 1200 \times (2 \times 10^{-5} \times e^{(4.460\times1000/T_K)}) (1 + (1.211 \times 2 \times 10^{-5} \times e^{(4.460\times1000/T_K)})\dot{\gamma})^{0.521})^{(0.349-1)/0.521}$
5.3	$\eta = 1400 \times (2 \times 10^{-5} \times e^{(4.271\times1000/T_K)}) (1 + (0.007 \times 2 \times 10^{-5} \times e^{(4.271\times1000/T_K)})\dot{\gamma})^{0.279})^{(0.546-1)/0.279}$
5.4	$\eta = 2700 \times (3 \times 10^{-5} \times e^{(4.215\times1000/T_K)}) (1 + (4.433 \times 3 \times 10^{-5} \times e^{(4.215\times1000/T_K)})\dot{\gamma})^{0.553})^{(0.362-1)/0.533}$

References

1. Sandia National Laboratory. Sandia polymer electrolyte membrane brings goal of a high temperature PEM fuel cell closer. Available at: http://www.sandia.gov/news-center/news-releases/2004/renew-energy-batt/microfuel.html, 2004 (accessed 2007).
2. Glenn Research Center. Polymer Membranes for High-temperature PEM Fuel Cells and Solid Polymer Batteries, article # M-1406-3. Available at: http://technology.grc.nasa.gov/tops/TOP300178.pdf, 2004 (accessed 2007).
3. Di Vona, M. L.; Marani, D.; D'Epifanio, A.; Traversa, E.; Trombetta, M.; Licoccia, S.; Caldarelli, S.; Knauth, P. Solid State Ionics 2005, 835, 235.
4. Hu, Z.; Yin, Y.; Kita, H.; Okamoto, K.-i.; Suto, Y.; Wang, H.; Kawasato, H. Polymer 2007, 48 1962.
5. Zawodzinski, T. High Temperature Polymer Membranes for Fuel Cells. Available at: www.eere.energy.gov/hydrogenandfuelcells/pdfs/review04/fc_6_zawodzinski.pdf, 2004 (accessed 2007).
6. Xiao, L. Novel Polybenzimidazole Derivatives for High Temperature Polymer Electrolyte Membrane Fuel Cell Applications, Department of Mechanical Aerospace and Nuclear Engineering, Rensselaer Polytechnic Institute Dissertation, 2003; p 1–176.
7. Xiao, L.; Zhang, H.; Jana, T.; Scanlon, E.; Chen, R.; Choe, E. W.; Ramanathan, L. S.; Yu, S.; Benicewicz, B. C. Fuel Cells 2005, 5, 287.
8. Appleby, A. J. J Power Sources 1996, 58, 153.
9. Wang, J. T.; Savinell, R. F.; Wainright, J.; Litt, M.; Yu, H. Electrochim Acta 1996, 41, 193.
10. Giordano, N.; Staiti, P.; Hocevar, S.; Arico, A. S. Electrochim Acta 1996, 41, 397.
11. Kreuer, K. D. Solid State Ionics 1997, 97, 1.
12. Savadogo, O.; Xing, B. J New Mater Electrochem Systems 2000, 3, 343.
13. Alberti, G.; Casciola, M.; Massinelli, L.; Bauer, B. J Membr Sci 2001, 185, 73.
14. Fuller, T. F.; Perry, M. L. J Electrochem Soc 2002, 149, 59.
15. Nakajima, H.; Nomura, S.; Sugimoto, T.; Nishikawa, S.; Honma, I. J Electrochem Soc 2002, 149, 953.
16. Johnson, A.; Flori, A. Proceedings of APEX, San Diego, California, 2001, p 13.
17. Jiang, Z.; Carroll, B.; Abraham, K. M. Electrochim Acta 1997, 42, 2667.
18. Jansen, J. C.; MacChione, M.; Oliviero, C.; Mendichi, R.; Ranieri, G. A.; Drioli, E. Polymer 2005, 46, 11366.
19. Ren, J.; Wang, R.; Zhang, H.-Y.; Li, Z.; Liang, D. T.; Tay, J. H. J Membr Sci 2006, 281, 334.
20. Harris, T. A. L.; Walczyk, D.; O'Donnell, R.; Puffer, R. Trans NAMRI/SME 2004, 32, 431.
21. Harris, T. A. L. Design Methodology, Science, and Technology to Manufacture High Temperature Polymer Electrolyte Membranes for Fuel Cells, PhD Thesis, Rensselaer Polytechnic Institute, Troy, NY, 2006.
22. Morrison, F. Understanding Rheology; Oxford University Press: New York, 2001; p 231–232.
23. Tobolsky, A. V. Properties and Structures of Polymers; Wiley: New York, 1960.
24. Ferry, J. D. Viscoelastic Properties of Polymers, 3rd ed.; Wiley: New York, 1980.
25. Skelland, H. P. Non-Newtonian Flow and Heat Transfer; Wiley: New York, 1967.
26. Rosato, D. V.; Rosato, D. V. Plastics Engineered Product Design; Elsevier: Oxford, UK, 2003.